

<sup>14</sup>Although we have not completely calculated the quantity in (13), general analysis of the difference in phase space for S-W and equipartitioned jets implies (for  $\delta, \epsilon$

small) the result given. Compare with (3) and (7).

<sup>15</sup>T. DeGrand, Y. Ng, and S. Tye, Phys. Rev. D **16**, 3251 (1977).

## Comparison of Fusion Cross Sections for $^{10}\text{B} + ^{16}\text{O} \rightarrow ^{26}\text{Al}$ and $^{12}\text{C} + ^{14}\text{N} \rightarrow ^{26}\text{Al}$

J. Gomez del Campo, R. A. Dayras,<sup>(a)</sup> J. A. Biggerstaff, D. Shapira, A. H. Snell,  
P. H. Stelson, and R. G. Stokstad

Oak Ridge National Laboratory, Oak Ridge, Tennessee 37830

(Received 15 March 1979)

The cross section for fusion of  $^{10}\text{B} + ^{16}\text{O}$  is found to differ markedly from that of  $^{12}\text{C} + ^{14}\text{N}$  for bombarding energies in the range 3 to 9 times the fusion barrier. This difference exceeds that expected on the basis of calculated or measured nuclear density distributions for these nuclei.

The cross section for fusion of complex nuclei,  $\sigma_{\text{fus}}$ , is determined by a delicate balance between nuclear, Coulomb, centrifugal, and dissipative forces. Macroscopic treatments of fusion based on the above considerations can account for the gross energy dependence of  $\sigma_{\text{fus}}$ .<sup>1-4</sup> In general, such models work very well for energies up to and just beyond  $E_B$ , where  $E_B$  denotes the fusion barrier. They account for a large body of experimental data with parameters which vary only slightly from case to case<sup>1-3</sup> or with parameters based on experimental measurements of charge distributions.<sup>4</sup> Some exceptions to this have been noted, viz. for  $p$ -shell and  $s$ - $d$ -shell targets at energies far below,<sup>5</sup> and just above,<sup>6-8</sup> the barrier. Deviations from the predictions of macroscopic models are taken as evidence for microscopic phenomena, i.e., for the influence of individual nucleons on  $\sigma_{\text{fus}}$  above and beyond their static contribution to the mean-nuclear-density and -interaction potential. Essential aspects of the search for and study of these microscopic effects are (i) the measurement of  $\sigma_{\text{fus}}$  over a wide energy range and (ii) the isolation of different factors which can affect fusion. Concerning the latter aspect, we refer to the relative influence of the entrance channel and the compound nucleus.<sup>9</sup> A classic study of this is the work of Zebelman and Miller<sup>10</sup> for reactions leading to the compound nucleus  $^{170}\text{Yb}$ . For light nuclei, however, there are very few measurements for which the maximum projectile energy exceeds 10 MeV/A, and none of these<sup>8, 11</sup> allows a comparison of different reactions populating the same compound nucleus. We report here new experimental data for the reaction  $^{10}\text{B} + ^{16}\text{O}$  and present

a comparison with  $^{12}\text{C} + ^{14}\text{N}$  (Refs. 12-14) over an energy range sufficiently wide in each case to probe the "liquid-drop limit"<sup>15</sup> for fusion. The surprising result is that  $\sigma_{\text{fus}}$  for  $^{10}\text{B} + ^{16}\text{O}$  is markedly different from that for  $^{12}\text{C} + ^{14}\text{N}$  in the energy region between  $\sim 3E_B$  and  $\sim 9E_B$ . This difference, which is as large as  $(41 \pm 15)\%$ , significantly exceeds that expected on the basis of measured or calculated charge densities for the reacting nuclei.

The method of determining  $\sigma_{\text{fus}}$  has been described previously.<sup>12-14</sup> The present measurements of the  $^{10}\text{B} + ^{16}\text{O}$  reaction covered the energy range from  $E_{c.m.} = 15$ –80 MeV in nine steps. Beams of  $^{16}\text{O}$  from the Oak Ridge Isochronous Cyclotron were used to bombard thin self-supporting foils of boron enriched to 98% in  $^{10}\text{B}$ . The cross sections for fusion and for peripheral reactions,  $\sigma_{\text{dir}}$ , are shown in Fig. 1. For  $E_{c.m.}$  energies up

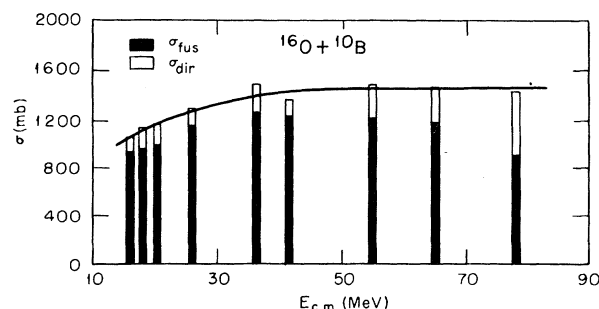


FIG. 1. Measured cross sections for the  $^{16}\text{O} + ^{10}\text{B}$  system. The solid histograms correspond to  $\sigma_{\text{fus}}$  and the open ones to  $\sigma_{\text{dir}}$ . The sum of these is to be compared with  $\sigma_R$  (solid line) calculated from an optical-model fit to elastic-scattering measurements.

to 36 MeV, the direct-reaction yield is concentrated (65%) in the oxygen isotopes. At the highest energy ( $E_{c.m.} = 78$  MeV) the relative direct-reaction yields are 9%, 42%, 17%, and 31% for the F, O, N, and C isotopes, respectively. The full curve in Fig. 1 is an optical-model calculation of the total reaction of the total reaction cross section,  $\sigma_R$ , derived from measurements of the elastic scattering. Since the identification of the evaporation residues is based on the different kinematic features of evaporation residues and products of peripheral reactions, a sensitive check on our procedures may be made by inverting the target and projectile. This was done in one case ( $E_{c.m.} = 41$  MeV) by bombarding a gaseous  $^{16}\text{O}$  target<sup>16</sup> with a  $^{10}\text{B}$  beam. A small amount of xenon (0.2%) was added to the gas to enable an absolute normalization based on Rutherford scattering. It may be seen in Fig. 1 that this measurement agrees well with measurements at adjacent energies. [The direct-reaction yield in this case appears low because  $^9\text{B}$  is particle unstable. The direct-reaction relative yields are 80%, 17%, and 3% for the B, C, and N isotopes, respectively.] The values of  $\sigma_R$  obtained from the optical model and those obtained by adding the independently measured values of  $\sigma_{fus}$  and  $\sigma_{dir}$  are in good agreement (Fig. 1). We note that the values of  $\sigma_R$  obtained for  $^{12}\text{C} + ^{14}\text{N}$  (Refs. 12-14) are

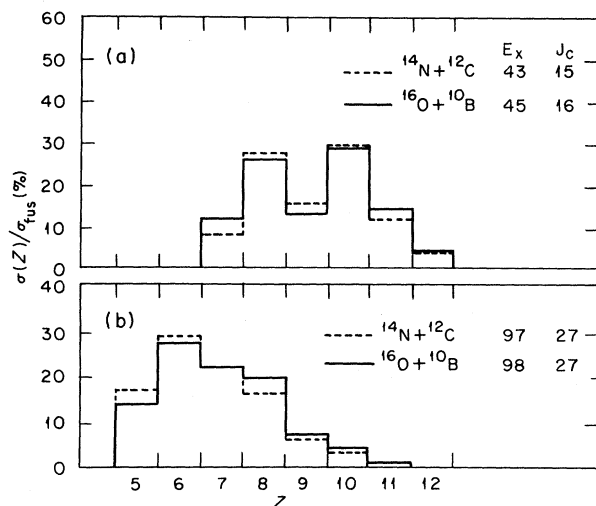


FIG. 2. Comparison of the angle-integrated yields of evaporation residues, for  $^{16}\text{O} + ^{10}\text{B}$  (present measurements) and  $^{14}\text{N} + ^{12}\text{C}$  (from Refs. 12-14) at (a) low and (b) high bombarding energies. The excitation energies (MeV) in  $^{26}\text{Al}$  and critical angular momenta (in units of  $\hbar$ ) are indicated.

very similar to those shown in Fig. 1.

Before one can eliminate the properties of the compound nucleus in a comparison of  $\sigma_{fus}$  for different entrance channels, it is important to verify that a compound system has been formed whose decay modes are independent of the entrance channel. Relative elemental yields of the evaporation residues are shown in Fig. 2. The similarities observed at both high and low bombarding energies suggest that the decay of the compound nucleus appears to be independent of whether it is formed by the reaction of  $^{10}\text{B} + ^{16}\text{O}$  or  $^{12}\text{C} + ^{14}\text{N}$ . We note also that statistical-model predictions<sup>17</sup> of these relative yields are in good agreement with the experimental results.

The values of  $\sigma_{fus}$  for  $^{10}\text{B} + ^{16}\text{O}$  are compared as a function of  $1/E_{c.m.}$  with previously measured values<sup>12-14</sup> for  $^{12}\text{C} + ^{14}\text{N}$  in Fig. 3. For bombarding energies up to  $E_{c.m.} = 20$  MeV ( $\approx 3E_B$ ), the cross sections are similar, as would be expected.<sup>1-3</sup> As bombarding energy increases, however, those for  $^{10}\text{B} + ^{16}\text{O}$  continue to increase, whereas they decline for  $^{12}\text{C} + ^{14}\text{N}$ . At the highest bombard-

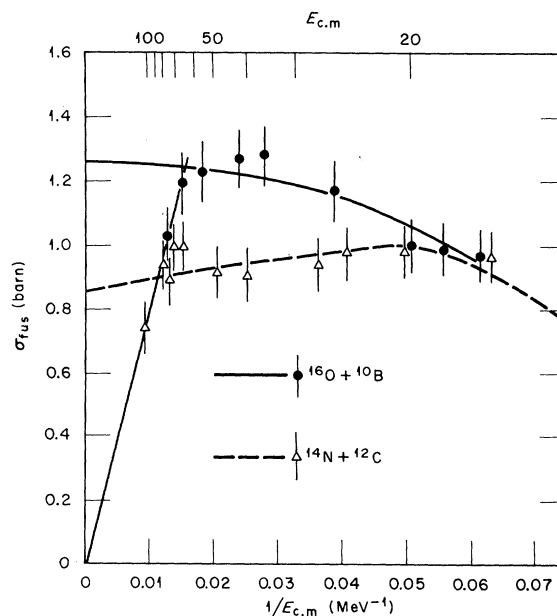


FIG. 3. The fusion cross section vs  $1/E_{c.m.}$ . The solid points are for  $^{16}\text{O} + ^{10}\text{B}$  (present measurements) and the open triangles for  $^{14}\text{N} + ^{12}\text{C}$  (from Refs. 12-14). The thick solid line and the dashed line are (Glas-Mosel) fits to the data for  $^{16}\text{O} + ^{10}\text{B}$  and  $^{14}\text{N} + ^{12}\text{C}$ , respectively, with the parameters given in the text. The thin solid line intersecting the origin gives the expected trend of  $\sigma_{fus}$  vs  $1/E_{c.m.}$  for a constant maximum angular momentum of  $27\hbar$ .

ing energies,  $\sigma_{\text{fus}}$  shows a rapid decrease. In fact, the two highest-energy points for both  $^{10}\text{B} + ^{16}\text{O}$  and  $^{12}\text{C} + ^{14}\text{N}$  lie on a straight line intersecting the origin (see Fig. 3). Since the reduced masses are equal (to within 5%), this result implies that  $\sigma_{\text{fus}}$  for both reactions is subject to the same energy-independent maximum angular momentum ( $J_{\text{max}} = 27\hbar$ ). It is thus reasonable to associate this angular momentum limit with the compound nucleus, as was suggested in Ref. 13, and not with the entrance channel. It was noted in Ref. 13 that  $27\hbar$  is the value for which the fission barrier is predicted to vanish<sup>15</sup> and for which an equilibrated compound nucleus would not be expected to be formed. Thus, the behavior of  $\sigma_{\text{fus}}$  at the lower energies and at the highest energies is as expected, at least on the basis of purely macroscopic considerations. In the first case, the similar values of  $A_1^{1/3} + A_2^{1/3}$  and  $Z_1 Z_2$  for the two reactions imply similar outer fusion barriers,<sup>3</sup>  $V_B$ , and radii,  $R_B$ ; in the second case, it is a macroscopic property of the compound nucleus which is responsible.

The remarkable feature of the comparison shown in Fig. 3 is the striking difference in magnitude of  $\sigma_{\text{fus}}$  in the energy region  $25 \leq E_{\text{c.m.}} \leq 65$  MeV. At one point,  $E_{\text{c.m.}} = 40$  MeV,  $\sigma_{\text{fus}}$  for  $^{10}\text{B} + ^{16}\text{O}$  exceeds that for  $^{12}\text{C} + ^{14}\text{N}$  by a factor of 1.41, i.e., by  $(41 \pm 15)\%$ . This difference is significantly larger than the typical difference observed at lower energies for systems which are similar but which do not lead to the same compound nucleus.<sup>6-8</sup> It exceeds by an even larger amount the differences expected on the basis of various macroscopic models. For example, the dashed line in Fig. 3 corresponds to the Glas-Mosel formula with the parameters  $r_B = 1.50$ ,  $V(R_B) = 6.7$ ,  $r_{\text{cr}} = 1.11$ ,  $V(R_{\text{cr}}) = -1.9$ ,  $\hbar\omega = 2$ , where the units are fm and MeV. If the values of  $V(R_{\text{cr}})$  and  $V(R_B)$  are readjusted slightly because of the 4% difference in the Coulomb potential and the other parameters are left unchanged, the prediction for  $^{10}\text{B} + ^{16}\text{O}$  deviates from the dashed line by at most 5% in the energy region shown in Fig. 3. Electron-scattering measurements and shell-model calculations demonstrate, however, that the half-density radii of nuclei in this mass region do not scale simply as  $A^{1/3}$ . For example, calculations of the nuclear density by Satchler, using the folding model of Satchler and Love,<sup>18</sup> indicate that  $^{12}\text{C} + ^{14}\text{N}$  and  $^{10}\text{B} + ^{16}\text{O}$  have the same mass overlap at radii of 1.11 and 1.15 times  $(A_1^{1/3} + A_2^{1/3})$ , respectively. Incorporating this in the Glas-Mosel formulation<sup>3</sup> produces a maximum predicted dif-

ference in the cross section of 7%, which accounts for only about  $\frac{1}{5}$  of the observed difference. The procedure suggested by Horn and Ferguson<sup>4</sup> is similarly unable to reproduce the observed effect. [The parameters which best reproduce the experimental data for  $^{16}\text{O} + ^{10}\text{B}$  are  $r_B = 1.5$ ,  $V_B(R_B) = 6.7$ ,  $r_{\text{cr}} = 1.35$ ,  $V(R_{\text{cr}}) = 2.5$ , and  $\hbar\omega = 2$  and correspond to the full curve in Fig. 3.] Thus, the effects of individual nucleonic motion on the density profiles of the constituent nuclei and on the conservative interaction potentials of the two systems cannot account for the experimental differences observed here.

Birkelund *et al.*<sup>19</sup> have shown quantitatively how the inclusion of a nonconservative potential in a dynamical model increases the cross section for fusion at high energies over the friction-free case. Within the context of their model, the qualitative question posed by the present experimental results is the following: Why are these dissipative forces so much stronger for  $^{10}\text{B} + ^{16}\text{O}$  than  $^{12}\text{C} + ^{14}\text{N}$ ? An answer to this question might be provided by microscopic calculations of inelastic processes within a two-center shell model, such as performed by Glas and Mosel<sup>20</sup> and by Von Charzewski *et al.*<sup>21</sup> The time-dependent Hartree-Fock approximation,<sup>22</sup> and the fragmentation theory,<sup>23</sup> as applied to heavy-ion collisions, are other microscopic approaches which might possibly account for the experimental results shown in Fig. 3.

Since we have shown that the total reaction cross sections for  $^{10}\text{B} + ^{16}\text{O}$  and  $^{12}\text{C} + ^{14}\text{N}$  are similar, the observed differences can be stated equivalently in terms of the direct-reaction cross sections, viz.  $\sigma_{\text{dir}}(^{12}\text{C} + ^{14}\text{N}) \approx 2 \sigma_{\text{dir}}(^{10}\text{B} + ^{16}\text{O})$  in the energy range of 40–70 MeV (c.m.). Since fusion can occur only after the nuclei have first experienced a peripheral overlap, microscopic theories of peripheral interactions<sup>24</sup> are also relevant for the questions raised by these experimental data.

In summary, we have shown that the formation of  $^{26}\text{Al}$  through the reactions  $^{10}\text{B} + ^{16}\text{O}$  and  $^{12}\text{C} + ^{14}\text{N}$  follows macroscopic expectations just above the fusion barrier and at the very high energies for which a "liquid-drop limit" is observed. The magnitude of  $\sigma_{\text{fus}}$  for  $^{10}\text{B} + ^{16}\text{O}$ , however, is strikingly and unexpectedly larger than that for  $^{12}\text{C} + ^{14}\text{N}$  at the intermediate energies and represents an interesting challenge for microscopic theories of heavy-ion reactions.

This research was sponsored by the U. S. Department of Energy. Oak Ridge National Laboratory is operated by Union Carbide Corporation for the U. S. Department of Energy.

<sup>(a)</sup>Present address: Service de Physique, Centre d'Etudes de Bruyeres-le-Chatel, B. P. No. 561, 92542 Montrouge, France.

<sup>1</sup>R. Bass, Nucl. Phys. **A231**, 45 (1974), and Phys. Rev. Lett. **39**, 265 (1977).

<sup>2</sup>J. Galin *et al.*, Phys. Rev. C **9**, 1018 (1974).

<sup>3</sup>D. Glas and U. Mosel, Nucl. Phys. **A237**, 429 (1975).

<sup>4</sup>D. Horn and A. J. Ferguson, Phys. Rev. Lett. **41**, 1529 (1978), and Nucl. Phys. **A311**, 238 (1978).

<sup>5</sup>R. G. Stokstad *et al.*, Phys. Rev. Lett. **37**, 888 (1976).

<sup>6</sup>P. Sperr *et al.*, Phys. Rev. Lett. **37**, 321 (1976).

<sup>7</sup>M. Conjeaud *et al.*, Nucl. Phys. **A309**, 515 (1978).

<sup>8</sup>D. G. Kovar, in Proceedings of the IPCR (Institute of Physical and Chemical Research) Symposium on Macroscopic Features of Heavy-Ion Collisions and Pre-Equilibrium Process, Hakone, Japan, 1977, edited by H. Kamitsubo and M. Ishihara (unpublished).

<sup>9</sup>D. Glas and U. Mosel, Phys. Lett. **78B**, 9 (1978).

<sup>10</sup>A. M. Zebelman and J. M. Miller, Phys. Rev. Lett. **30**, 27 (1973).

<sup>11</sup>M. N. Namboodiri *et al.*, Nucl. Phys. **A263**, 491 (1976).

<sup>12</sup>R. G. Stokstad *et al.*, Phys. Rev. Lett. **36**, 1529 (1976).

<sup>13</sup>R. G. Stokstad *et al.*, Phys. Lett. **70B**, 289 (1977).

<sup>14</sup>J. Gomez del Campo *et al.*, Phys. Rev. C **19**, 2170 (1979).

<sup>15</sup>S. Cohen *et al.*, Ann. Phys. (N.Y.) **82**, 557 (1974).

<sup>16</sup>D. Shapira *et al.*, to be published.

<sup>17</sup>J. Gomez del Campo and R. G. Stokstad, Monte Carlo Hauser-Feshbach Code LILITA.

<sup>18</sup>R. Satchler and W. G. Love, Phys. Lett. **65B**, 415 (1976).

<sup>19</sup>J. R. Birkelund *et al.*, Phys. Rev. Lett. **40**, 1123 (1978).

<sup>20</sup>D. Glas and U. Mosel, Phys. Lett. **49B**, 301 (1974).

<sup>21</sup>C. Von Charzewski *et al.*, Nucl. Phys. **A307**, 309 (1978).

<sup>22</sup>P. Bonche *et al.*, Phys. Rev. C **17**, 1700 (1978); R. Y. Cusson *et al.*, Phys. Rev. C **18**, 2589 (1978).

<sup>23</sup>K. H. Ziegenhain *et al.*, Fisica **9**, 559 (1977).

<sup>24</sup>T. Tamura *et al.*, Phys. Lett. **66B**, 109 (1977).

## Determination of the Hyperfine Structure in the $A^2\Sigma_{1/2}^+$ State of OH by Frequency-Doubled Dye-Laser Radiation

J. J. ter Meulen, G. W. M. van Mierlo, and A. Dymanus

*Fysisch Laboratorium, Katholieke Universiteit, Toernooiveld, Nijmegen, The Netherlands*

(Received 5 February 1979)

The hyperfine structure of OH in the  $A^2\Sigma_{1/2}^+$  state has been measured by exciting a molecular beam with cw intracavity frequency-doubled dye-laser radiation. The splittings are 778 MHz for  $N' = 0$  and 200 to 500 MHz for  $1 \leq N' \leq 5$ . The values for the hyperfine and  $\rho$  doubling are  $b + \frac{1}{3}c = 777.8 \pm 2.0$  MHz,  $c = 165.8 \pm 2.8$  MHz, and  $\gamma = 7.13 \pm 0.03$  GHz. Also the hyperfine splitting of OD in the  $N' = 0$  state has been measured yielding  $b + \frac{1}{3}c = 119 \pm 2$  MHz.

The hydroxyl radical (OH) is one of the fundamental molecules in chemistry, physics, and astrophysics. It is the simplest diatomic open-shell system, readily accessible for a wide range of spectroscopic techniques (optical,<sup>1</sup> infrared,<sup>2</sup> microwave,<sup>3</sup> and molecular beam-maser and -resonance<sup>4,5</sup>) and accurate calculations. The radical plays an important role in laboratory and atmospheric chemistry and its maser emission in interstellar clouds forms a major unsolved problem in astrophysics.

In the past considerable effort has been spent to unravel the structure and properties of OH. The structure of the ground electronic state ( $X^2\Pi$ ), its vibrational and rotational levels, the  $\rho$  doubling, and the hyperfine structure are all well known.<sup>6</sup> This is, however, not the case for the first excited electronic state  $A^2\Sigma_{1/2}^+$  where only the rotational and  $\Lambda$ -doubling energies are

known from old optical work. The hyperfine structure due to the interaction between the magnetic moment  $I = \frac{1}{2}$  of the hydrogen nucleus and the electronic spin has not been measured yet. In level-crossing experiments German *et al.*<sup>7,8</sup> determined the hyperfine structure of OD in the  $A^2\Sigma_{1/2}^+$  state from which they calculated the splittings for OH. The estimated values are on the order of 300 MHz which is beyond the resolution of conventional Doppler-limited spectroscopy (4 GHz at 300 K).

The knowledge of the hyperfine structure is important not only for a theoretical understanding of the excited structure but also for the uv excitation models of interstellar OH radicals. As proposed by Litvak *et al.*,<sup>9</sup> uv pumping might cause a population inversion between the  $\Lambda$ -doublet levels in the rotational ground state  $^2\Pi_{3/2}$ ,  $J = \frac{3}{2}$ , leading to the observed maser emissions. Turner<sup>10</sup> has